frontiers in Materials

ORIGINAL RESEARCH
published: 06 July 2021
doi: 10.3389/fmats.2021.699579

The Effect of Antibacterial and Waterproof Coating Prepared From Hexadecyltrimethoxysilane and Nano-Titanium Dioxide on Wood Properties

Lechen Yang[1,2], *Yan Wu*[1,2]*, *Feng Yang*[3]* *and Wenhao Wang*[1,2]

[1]College of Furnishings and Industrial Design, Nanjing Forestry University, Nanjing, China, [2]Co-Innovation Center of Efficient Processing and Utilization of Forest Resources, Nanjing Forestry University, Nanjing, China, [3]Fashion Accessory Art and Engineering College, Beijing Institute of Fashion Technology, Beijing, China

As one of the most sustainable resources, wood has been widely used in the fields of construction, decoration, flooring and furniture. However, the micron-scale porous structure of wood makes it have strong moisture absorption capacity and is susceptible to bacterial adhesion. In order to expand its utility in more applications of wood products, it is necessary to make the wood have a certain antibacterial and waterproof properties. This study demonstrates a method of using hexadecyltrimethoxysilane and nano-titanium dioxide to prepare antibacterial and waterproof coating and apply it to wood surfaces. Studies have shown that this kind of wood coated with an antibacterial waterproof coating has excellent antibacterial properties (antibacterial rate as high as 99%) and waterproof properties. In addition, this antibacterial and waterproof coating does not cause a major change in the color of the wood, and at the same time increase the tensile strength and hardness to a certain extent. The above-mentioned properties of this antibacterial and waterproof coating provide a new idea for the preparation of wood coatings.

Keywords: coating, wood surface, antibacterial, waterproof, color difference, mechanical performance

OPEN ACCESS

Edited by:
Changdong Gu,
Zhejiang University, China

Reviewed by:
Aditya Kumar,
Indian Institute of Technology Dhanbad, India
Sudagar. J,
VIT-AP University, India

***Correspondence:**
Yan Wu
wuyan@njfu.edu.cn
Feng Yang
yangfeng@bift.edu.cn

Specialty section:
This article was submitted to Environmental Degradation of Materials, a section of the journal Frontiers in Materials

Received: *26 April 2021*
Accepted: *28 June 2021*
Published: *06 July 2021*

Citation:
Yang L, Wu Y, Yang F and Wang W (2021) The Effect of Antibacterial and Waterproof Coating Prepared From Hexadecyltrimethoxysilane and Nano-Titanium Dioxide on Wood Properties. Front. Mater. 8:699579. doi: 10.3389/fmats.2021.699579

INTRODUCTION

As a natural, biodegradable, recyclable and cheap material, wood is widely used in construction, decoration, furniture and other fields (Aigbomian and Fan, 2013; Zhu et al., 2016; Chen et al., 2017; Goodman et al., 2018). However, wood is not as dense as metal, it has a large number of pipe holes and gaps on its surface and inside, which makes it easy to be contaminated by different liquids and suffer from the adhesion of bacteria (Avramidis et al., 2009; Pouzet et al., 2018). Due to the porous structure and anisotropic characteristics of the wood, the wood can cause different degrees of wet swelling and drying shrinkage in all directions as the environmental humidity changes, which will cause the wood to crack or warp during use. For hundreds of years, people have been working to improve the properties of wood (Wang and Cooper, 2005; Humar et al., 2017; Chang et al., 2019). The usual solution is to coat wood with lacquer, wax or oil. The lacquer protection method is to cover the surface of the wood with a layer of airtight lacquer film to isolate the moisture and bacteria from the wood itself. However, most of the traditional lacquers are chemical products that are rich in

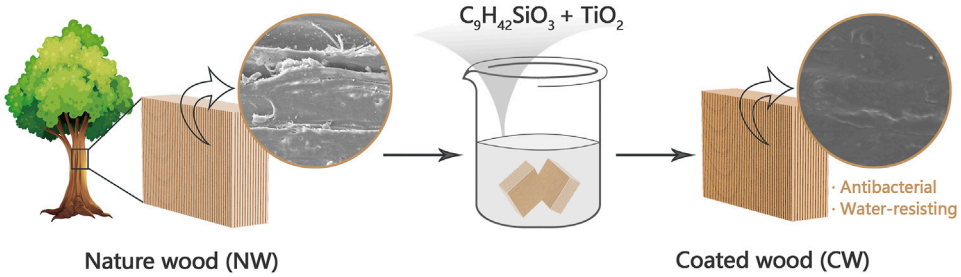

FIGURE 1 | Graphic illustration of the coated wood made from natural wood.

chemical substances harmful to the human body. Today, when we are concerned about green environmental protection, they are not favored. The main components of wax are fats formed by higher fatty acids and higher monohydric alcohols, which have certain effects in preventing rot and insects, but its waterproof performance is not excellent. The oil film applied to the wood can form a closed protection for the wood like the lacquer film, but the oil film has a strong smell and is difficult to disperse.

In recent years, more and more researches have focused on antibacterial and hydrophobic fields. Schoenfisch et al.(Privett et al., 2011) synthesized a superhydrophobic gel coating that significantly inhibited the adhesion of *Staphylococcus aureus* and *Pseudomonas aeruginosa*. Poncin-Epaillard et al. (2013) have created a highly hydrophobic polymer surface that reduces the adhesion of Gram-positive and negative pathogens. (Thakur et al. (2016) used eugenol laccase biografting to modify the fiber surface to develop fiber-reinforced polymer composites with antibacterial and hydrophobic functions. Bains et al. (2020) developed a hydrophobic coating material based on ionic liquid (IL) functionalized multi-walled carbon nanotubes (MWCNTs), which has certain antibacterial properties against *Staphylococcus aureus* and *Escherichia coli*. Kumar et al. (Pandit et al., 2020; Tudu et al., 2020a, 2020b) used titanium dioxide nanoparticles and perfluorooctyltriethoxysilane (PFOTS) as raw materials to successfully prepare superhydrophobic coatings on the surface of wood, cotton fabric and galvanized steel mess. Wu et al. (2021) prepared a super-hydrophobic antibacterial surface on cotton fabrics using UV-curable water-based paint, silver nanoparticles and stearic acid. As mentioned above, these coatings can all achieve super-hydrophobic function. However, the superhydrophobicity comes from the micro-nano structure on the surface: every micrometer mastoid is attached with countless nano-scale wax crystal particles (Xin and Hao, 2010; Yao et al., 2011; Barthlott and Neinhuis, 1997). This micro-nano structure significantly increases the contact angle of the surface, but it is also easy to make the surface become uneven. As we all know, wood usually requires a smooth surface in specific wood products or furniture applications, which makes many super-hydrophobic structure unsuitable for wood surfaces. In addition, previous research on superhydrophobic coatings on wood surfaces mainly focused on self-cleaning, anti-corrosion and oil-water separation properties (Shah et al., 2017; Huang et al., 2018; Jia S. et al., 2018), few reports have studied the effects of coatings on wood properties in detail, including antibacterial properties, surface color changes, and mechanical properties.

Here, we show a simple method of using hexadecyltrimethoxysilane ($C_9H_{42}SiO_3$) and nano-titanium dioxide (TiO_2) to prepare an antibacterial waterproof coating, and then coating it on natural wood (NW) to obtain coated wood (CW) (**Figure 1**). As a semiconductor material with photocatalytic function, nano-titanium dioxide has the advantages of high activity, good stability, low price, and good antibacterial effect, so it is widely used in air purification, self-cleaning and antibacterial fields (Montazer et al., 2011). Hexadecyltrimethoxysilane as a silane monomer contains a certain length of carbon chain, can significantly increase the water resistance of the wood surface (Xu et al., 2015; Zhang et al., 2020). In order to further study the effect of this antibacterial waterproof coating on wood, we conducted a series of analysis and characterization. The results show that compared with NW, CW not only has excellent antibacterial and waterproof functions, but also has no obvious surface color change, while obtaining higher tensile strength and hardness.

MATERIALS AND METHODS

Materials and chemicals

Beech wood (*Fagus Sylvatica*) was used as the base material of antibacterial waterproof coating, which was provided by Yihua Life Technology Co., Ltd. (Shantou, China). The hexadecyltrimethoxysilane in the experiment was purchased from Shanghai Macklin Biochemical Co., Ltd., China.; nano titanium dioxide was provided by Shanghai Aladdin Biochemical Technology Co., Ltd., China; and ethanol was purchased from Nanjing Chemical Reagent Co., Ltd., China. All of the chemicals used were of analytical grade.

The preparation process of wood coated with antibacterial and waterproof coating

First, a natural wood samples were cut into wood film (6 cm × 3 cm × 1 cm). Then the wood samples were ultrasonically cleaned with ethanol for 15 min to remove impurities, and subsequently were dried at 80°C for 5 h to obtain a wood sample in an absolutely dry state. After many experiments, it is finally

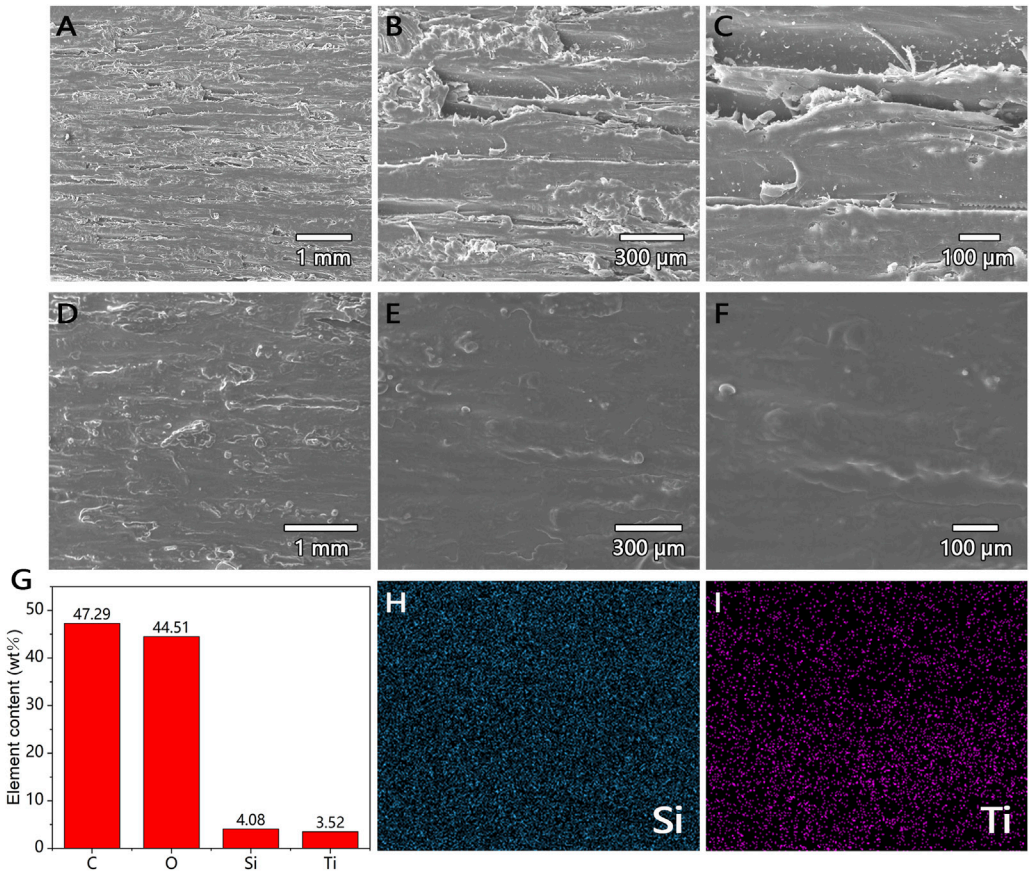

FIGURE 2 | The microscopic appearance of NW and CW. **(A–C)** SEM images of NW surface. **(D–F)** SEM image of the CW surface, showing the coating on the surface. **(G)** Relative element content of CW. **(H–I)** Energy dispersive X-ray spectroscopic maps shows the element distribution of Si and Ti on the CW surface.

determined that hexadecyltrimethoxysilane and ethanol are mixed in a ratio of (0.5–1):1, and then 1.5% titanium dioxide is added to the mixed solution (the best antibacterial effect is achieved when the titanium dioxide mass fraction is 1.5%), and stir it evenly with an ultrasonic dispersion mixer to obtain an antibacterial and waterproof reagent. Use a high-pressure electric sprayer to evenly spray the antibacterial and waterproof reagent on the surface of the natural wood samples to form a coating, and then dry it in a blast dryer at 80°C for 3 h to obtain a wood coated with an antibacterial and waterproof coating.

Measurements and characterization

A FEI Quanta 200 scanning electron microscope (SEM) equipped with an energy dispersive X-ray spectroscopic detector for mapping were used to observe the morphology and structure of the sample under an accelerating voltage of 30 kV. The fourier transform infrared spectrometer (VERTEX 80V, from Bruker Co., Ltd., Germany) was used to measure the FT-IR spectrum. XRD was measured on a Rigaku Ultima IV equipped with a curved detector manufactured by Rigaku Americas Corp. The water contact angles (CAs) were measured with a Contact Angle System OCA20 (CAs, from Krusch Scientific Instruments Co., Ltd., China). Use a colorimeter (RM200, from X-Rite Co., Ltd., United States) to measure the surface color of NW and CW under D65 standard light source. Measure the hardness with a Shore hardness tester (LX-D). The mechanical performance of the samples were evaluated using a universal testing machine (AG-IC 100KN, from SHIADAZU Co., Ltd., Japan).

RESULTS AND DISCUSSION

Morphology Analysis

The SEM images can clearly see the microscopic features of the NW and CW surfaces. **Figures 2A–F** are the SEM images of the NW and CW at different magnifications, respectively. Scanning electron microscopy results show that the surface of NW is relatively uneven, and some wood holes are exposed on the surface, and there are many burrs (NW only has a simple cutting process and no further polishing process). After coated with antibacterial and waterproof reagent, the microstructure of the wood surface has changed significantly. It can be seen that the CW surface is covered with a layer of coating, and the holes that were originally exposed on the wood surface are filled in (**Figures 2A,D**). And correspondingly, it can be seen from the comparison between **Figures 2B,E** that the surface of the wood has become

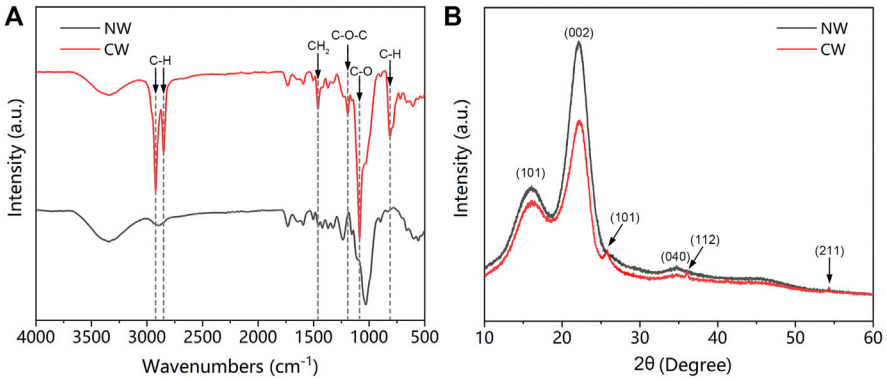

FIGURE 3 | Comparison of the chemical structure of NW and CW. **(A)** FT-IR spectra of the NW and CW. **(B)** XRD patterns of the NW and CW.

relatively flat and tidy. The main chemical components that make up wood are cellulose, hemicellulose and lignin, all of which are organic compounds and contain polar functional groups. In the interior of the wood, due to the intermolecular forces, these polar groups can attract each other to reach an equilibrium state. However, the molecules on the surface of the wood are still polar and have a certain surface free energy, which enables them to be well combined with the antibacterial waterproof coating (Ye et al., 2017; Teacă and Tanasa, 2020). The element content and element distribution diagrams of CW further prove this point (**Figures 2G–I**). The energy dispersive X-ray spectrum shows that Si element representing hexadecyltrimethoxysilane and Ti element representing nano-titanium dioxide are uniformly distributed on the surface of CW, and the relative element content of Si and Ti are 4.08 and 3.52%, respectively.

Chemical Structure Analysis

The Fourier transform infrared spectrum (FTIR) and X-ray diffraction (XRD) pattern of NW and CW can reflect the changes of internal chemical structure from the side. **Figure 3A** is the FTIR image of NW and CW, and the characteristic absorption peaks of wood are almost the same, including 3345 cm^{-1} (O-H stretch), 1733 cm^{-1} (C = O stretch, molecular motion of hemicellulose), 1,593 cm^{-1} and 1,505 cm^{-1} (aromatic skeleton vibration, molecular movement of lignin), 1,235 cm^{-1} (C-O stretch), 1,034 cm^{-1} (C-H stretch) and other absorption peaks, which indicate the chemical structure of the CW wood has not been damaged (Wu et al., 2020a; Yang et al., 2021). At the same time, the FTIR of CW also showed the characteristic absorption peaks of 2,915 cm^{-1} and 2,850 cm^{-1} (C-H stretch), 1,465 cm^{-1} (CH_2 bend) and 815 cm^{-1} (C-H bend) representing alkanes, which is mainly caused by the hexadecyltrimethoxysilane component in the coating. In addition, the ethanol component in the coating also caused the infrared spectrum of CW to show characteristic absorption peaks at 1,168 cm^{-1} (C-O-C stretch) and 1,091 cm^{-1} (C-O stretch).

Figure 3B is the XRD spectra of NW and CW, indicating that the positions of the main diffraction peaks of NW and CW are almost the same, both at 2θ = 16.2° (101 crystal plane), 22.3° (002 crystal plane), 34.8° (040 crystal plane), At the same time, the diffraction peaks around 2θ = 18° all indicate the diffraction intensity of the amorphous region (Huang et al., 2019; Yang et al., 2019). This is a typical characteristic diffraction peak of type I cellulose structure, indicating that the crystal structure of cellulose in CW does not change much. Among them, the diffraction peak intensity of CW at 2θ = 16.2° and 22.3° is lower than that of NW, because the coating on the surface of CW reduces the exposure of crystal planes. CW also has diffraction peaks at 2θ = 25.6° (101 crystal plane), 36.2° (112 crystal plane), and 54.5° (211 crystal plane), which are typical

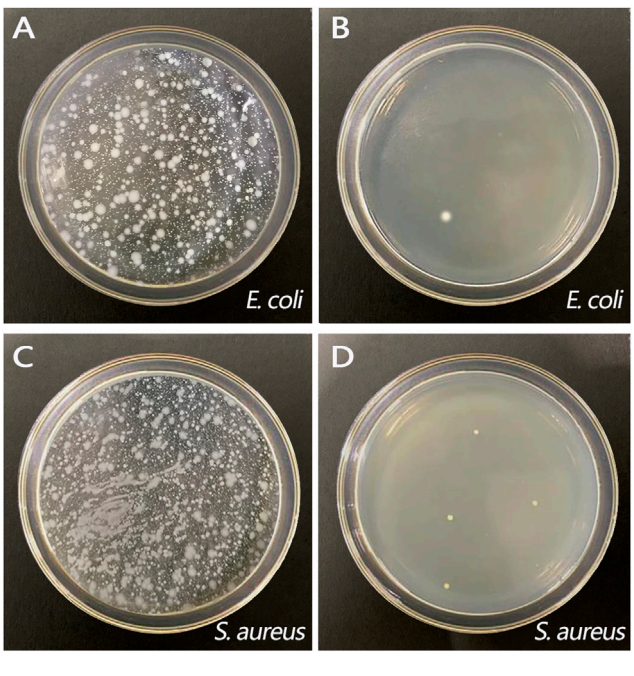

FIGURE 4 | Digital images of antibacterial activity of NW and CW. **(A)** Digital image of NW antibacterial activity against *Escherichia coli*. **(B)** Digital image of NW antibacterial activity against *Staphylococcus aureus*. **(C)** Digital image of CW antibacterial activity against *Escherichia coli*. **(D)** Digital image of CW antibacterial activity against *Staphylococcus aureus*.

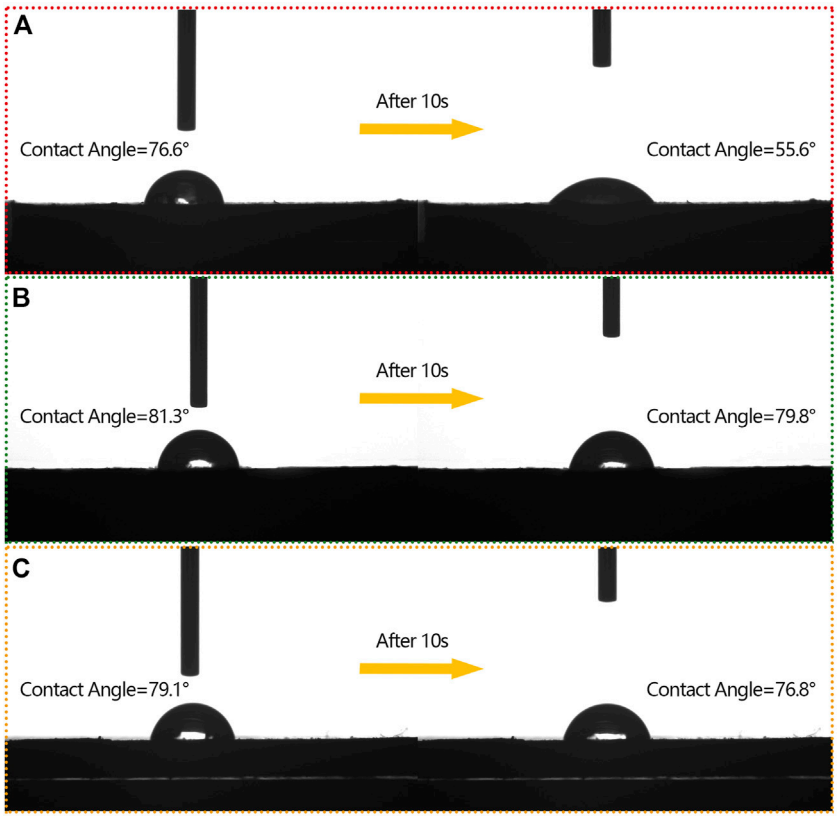

FIGURE 5 | The image of water contact angle test on NW and CW surface. **(A)** Image of the water contact angle of NW at the initial time and 10 s later. **(B)** Image of the water contact angle of CW at the initial time and 10 s later. **(C)** Image of the water contact angle of CW immersed in water.

diffraction peaks of TiO2. Combining the infrared spectra of NW and CW, it can be seen that the antibacterial waterproof coating does not affect the internal chemical structure of the wood, which ensures the good physical and chemical properties of the wood itself.

Antibacterial Property

In order to determine the antibacterial activity of the coating prepared by hexadecyltrimethoxysilane and nano-titanium dioxide, the antibacterial activity test was carried out in accordance with GB/T 21,866–2008 "Antibacterial Coating (Paint Film) Antibacterial Activity and Antibacterial Effect". In this experiment, Gram-negative *Escherichia coli* and Gram-positive *Staphylococcus aureus* were selected as the test bacteria, and the experimental results are shown in **Figure 4**. It can be seen from **Figures 4A,C** that NW has almost no antibacterial activity against *Escherichia coli* and *Staphylococcus aureus*, and the bacterial colonies almost cover the entire Petri dish. In sharp contrast, CW has excellent antibacterial properties, and there are only a few live bacteria in the corresponding Petri dishes (**Figures 4B,D**), and the antibacterial rate is as high as 99%. The main reason why CW is antibacterial is that its coating contains a certain amount of titanium dioxide. When titanium dioxide is excited by a certain energy of photons, it will undergo a photocatalytic reaction and produce many strong oxidizing substances, including hydroxyl radicals (OH), superoxide ion (O_2^-), hydrogen peroxide (H_2O_2) (Montazer et al., 2011). These active oxides can react with the cell components of microorganisms to decompose them into carbon dioxide and water, thereby killing bacteria in a short time to achieve antibacterial effects.

Waterproof Property

Figure 5 shows the water contact angle of the wood surface before and after the antibacterial waterproof reagent is coated, noting that CW has better water resistance than NW. When the water droplet first touched the NW surface, the contact angle formed was 76.6°. However, after only 10 s, the water droplet was quickly absorbed by the NW and formed a flat shape, and the contact angle dropped to 55.6° (**Figure 5A**). As a solid material that is easy to wet, the cell wall of wood is mainly composed of microcrystals, microfibrils, and fibrils. These components have gaps between each other and are connected to each other to form the microcapillary system of the wood, so its surface is convenient for the absorption and conduction of multiple liquids (Fu et al., 2018; Lin et al., 2018). After being coated with an antibacterial and waterproof reagent, the water absorption of the wood has reduced to a certain extent. As shown in **Figure 5B**, the initial water contact angle of CW is 81.3°, and it only drops by 1.5° after 10 s, which proves the good water resistance of CW. Since it is not

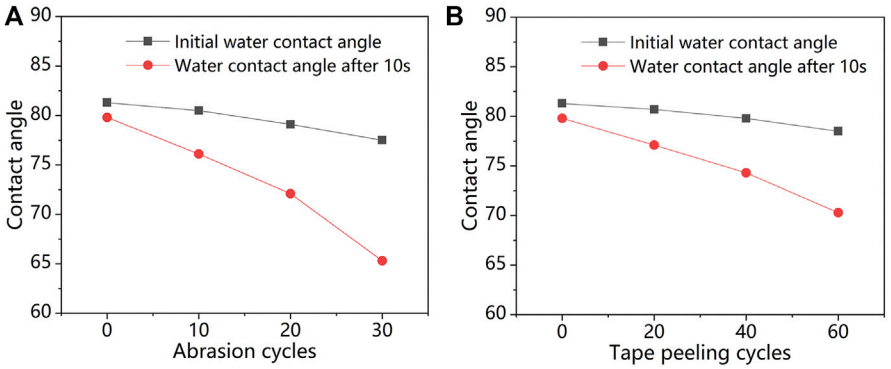

FIGURE 6 | Mechanical stability of CW coating. **(A)** Water contact angle of CW under different abrasion cycles. **(B)** Water contact angle of CW under different tape peeling cycles.

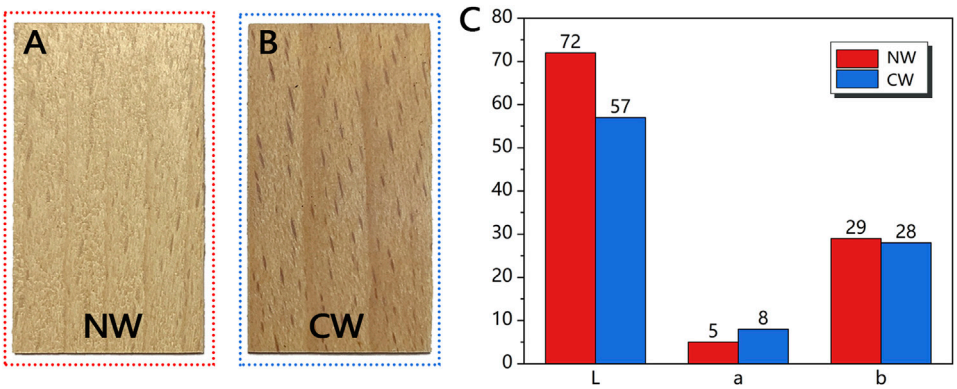

FIGURE 7 | Color change of NW and CW. **(A)** Digital image of NW. **(B)** Digital image of CW. **(C)** L, a, b values of NW and CW.

certain that the coating on the surface of CW can still maintain excellent waterproof performance after encountering water, we estimate the adhesion of the coating by immersing the CW sample in water and maintaining a certain stirring time. **Figure 5C** is an image of the water contact angle measured after the CW is stirred in water for 10 min and then dried naturally. It can be seen that the initial contact angle of the CW after stirred with water is only 2.2° lower than that of the CW without water stirred, indicating the good adsorption between the coating and the wood.

The mechanical stability of the coating is critical to the waterproof property of CW. The mechanical stability of the coating was tested by cyclically rubbing the sample on 1,000 # sandpaper and repeatedly peeling off the tape on the CW surface. **Figure 6A** shows the results of the water contact angle corresponding to the abrasion test of the CW coating. It was observed that within 20 cycles, the water contact angle of CW dropped by less than 10°, indicated the abrasive resistance of the coating. After 30 cycles, the coating was destroyed and the water contact angle dropped significantly. In the tape peeling test, after up to 60 peeling cycles, the water contact angle of CW decreased within 10°, showed the adhesive strength of the coating (**Figure 6B**).

Color Difference Analysis

After finishing with antibacterial and waterproof coating, the surface color of wood will change to a certain extent. In order to more intuitively characterize the color change of CW relative to NW, the International Organization for Standardization (ISO) CIE $L^*a^*b^*$ (1976) standard colorimetric characterization system is used to quantitatively characterize the color to analyze its color Variety (Colorimetry-Part C.I.E, 4, 1976). The ΔL^* value represents the change in the degree of brightness of the sample, when the value is positive, the sample becomes brighter, and when the value is negative, the sample becomes darker; The Δa^* value represents the red-green change of the sample, a positive value means red, and a negative value means green; The Δb^* value represents the yellow-blue change of the sample, a positive value represents yellow, and a negative value represents blue (Wu et al., 2020b). From the digital images of NW and CW, it can be seen that the color of CW is slightly darker and the wood texture is clearer (**Figures 7A,B**). The NW and CW corresponding L, a, and b values are shown in **Figure 7C**. In terms of brightness, the value of L from NW to CW decreases significantly, and ΔL^* is 15. While in the red-green color represented by the a value and the yellow-green color represented by the b value, CW showed only small changes, with Δa^* and Δb^*

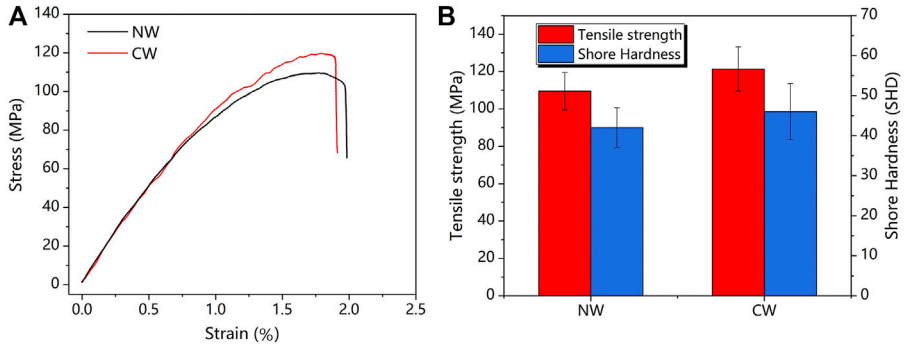

FIGURE 8 | Comparison of mechanical properties of NW and CW. **(A)** Representative stress-strain curves of NW and CW. **(B)** The tensile strength and shore hardness of NW and CW.

being 3 and 1, respectively. The total color difference ΔE^{*}_{ab} is about 15.33, and the ΔE^{*}_{ab} value is calculated according to **eq. 1**.

$$\Delta E^{*}_{ab} = \sqrt{(\Delta L^{*})^2 + (\Delta a^{*})^2 + (\Delta b^{*})^2} \quad (1)$$

Mechanical Performance

Good mechanical properties are essential for the practical application of CW, so CW is further evaluated through mechanical tensile test and hardness test. The tensile experiment was carried out using a computer-controlled electronic universal testing machine. After several pre-treatments, it was determined that the load was applied at a speed of 2 mm/min until the sample was stretched to break. Record the data to get the stress-strain curve and tensile strength of NW and SW. At the same time, used the Shore hardness tester (LX-D) to measure the hardness of NW and CW. **Figure 8A** shows the representative stress-strain curves of NW and CW. It can be seen that CW can withstand higher stress than NW, but the strain produced is less than NW. Through the coating of antibacterial and waterproof reagent, CW obtained higher tensile strength and surface hardness, which were 121.3 MPa and 46 SHD, respectively, which were better than NW's 109.5 MPa and 42 SHD (**Figure 8B**). The high tensile strength of CW can be attributed to the reason that the coating makes its surface structure denser, which makes CW consume more energy during the stretching process, resulting in higher mechanical tensile strength (Jia C. et al., 2018). At the same time, the coating also made the surface hardness of CW slightly increased, showing the positive impact of the antibacterial waterproof coating on the mechanical properties of wood.

CONCLUSIONS

In summary, we have successfully prepared an antibacterial waterproof coating through hexadecyltrimethoxysilane and nano-titanium dioxide that can be applied to natural wood. This is a simple, low-cost and efficient process, which provides a new idea for the preparation of wood coatings. The research results show that this kind of coating with good adsorption to wood can not only bring up to 99% antibacterial rate to the material, but also has excellent waterproof function. In addition, it will not bring significant color changes to the wood, and it can also optimize the mechanical properties of the wood and increase its tensile strength and hardness. This simple, top-down method can easily produce antibacterial and waterproof wood, which is expected to open up a series of new possibilities in the fields of wood products, furniture and interior decoration.

DATA AVAILABILITY STATEMENT

The raw data supporting the conclusions of this article will be made available by the authors, without undue reservation.

AUTHOR CONTRIBUTIONS

All authors listed have made a substantial, direct, and intellectual contribution to the work and approved it for publication.

FUNDING

The authors gratefully acknowledge the financial support from the project funded by the National Natural Science Foundation of China (32071687 and 32001382), the Project of Science and Technology Plan of Beijing Municipal Education Commission (KM202010012001), and the Special Scientific Research Fund of Construction of High-level teachers Project of Beijing Institute of Fashion Technology (BIFTQG201805).

REFERENCES

Aigbomian, E. P., and Fan, M. (2013). Development of Wood-Crete Building Materials from Sawdust and Waste Paper. *Construction Building Mater.* 40, 361–366. doi:10.1016/j.conbuildmat.2012.11.018

Avramidis, G., Hauswald, E., Lyapin, A., Militz, H., Viöl, W., and Wolkenhauer, A. (2009). Plasma Treatment of wood and wood-based Materials to Generate Hydrophilic or Hydrophobic Surface Characteristics. *Wood Mater. Sci. Eng.* 4, 52–60. doi:10.1080/17480270903281642

Bains, D., Singh, G., Bhinder, J., Agnihotri, P. K., and Singh, N. (2020). Ionic Liquid-Functionalized Multiwalled Carbon Nanotube-Based Hydrophobic Coatings for Robust Antibacterial Applications. *ACS Appl. Bio Mater.* 3, 2092–2103. doi:10.1021/acsabm.9b01217

Barthlott, W., and Neinhuis, C. (1997). Purity of the Sacred lotus, or Escape from Contamination in Biological Surfaces. *Planta* 202, 1–8. doi:10.2307/23384993

Chang, C.-W., Lee, H.-L., and Lu, K.-T. (2019). Manufacture and Characteristics of Oil-Modified Refined Lacquer for wood Coatings. *Coatings* 9, 11–12. doi:10.3390/coatings9010011

Chen, C., Li, Y., Song, J., Yang, Z., Kuang, Y., Hitz, E., et al. (2017). Highly Flexible and Efficient Solar Steam Generation Device. *Adv. Mater.* 29, 1701756. doi:10.1002/adma.201701756

Colorimetry-Part C. I. E. 4 (1976). *L* a* B* Colour Space*. (ISO 11664-4: 2008).

Fu, Q., Ansari, F., Zhou, Q., and Berglund, L. A. (2018). Wood Nanotechnology for Strong, Mesoporous, and Hydrophobic Biocomposites for Selective Separation of Oil/Water Mixtures. *ACS Nano* 12, 2222–2230. doi:10.1021/acsnano.8b00005

Goodman, S. M., Bura, R., and Dichiara, A. B. (2018). Facile Impregnation of Graphene into Porous Wood Filters for the Dynamic Removal and Recovery of Dyes from Aqueous Solutions. *ACS Appl. Nano Mater.* 1, 5682–5690. doi:10.1021/acsanm.8b01275

Huang, C., Su, Y., Shi, J., Yuan, C., Zhai, S., and Yong, Q. (2019). Revealing the Effects of Centuries of Ageing on the Chemical Structural Features of Lignin in Archaeological Fir Woods. *New J. Chem.* 43, 3520–3528. doi:10.1039/c9nj00026g

Huang, J., Wang, S., Lyu, S., and Fu, F. (2018). Preparation of a Robust Cellulose Nanocrystal Superhydrophobic Coating for Self-Cleaning and Oil-Water Separation Only by Spraying. *Ind. Crops Prod.* 122, 438–447. doi:10.1016/j.indcrop.2018.06.015

Humar, M., Kržišnik, D., Lesar, B., Thaler, N., Ugovšek, A., Zupančič, K., et al. (2017). Thermal Modification of Wax-Impregnated wood to Enhance its Physical, Mechanical, and Biological Properties. *Holzforschung* 71, 57–64. doi:10.1515/hf-2016-0063

Jia, C., Chen, C., Kuang, Y., Fu, K., Wang, Y., Yao, Y., et al. (2018a). From Wood to Textiles: Top-Down Assembly of Aligned Cellulose Nanofibers. *Adv. Mater.* 30, 1801347. doi:10.1002/adma.201801347

Jia, S., Chen, H., Luo, S., Qing, Y., Deng, S., Yan, N., et al. (2018b). One-step Approach to Prepare Superhydrophobic wood with Enhanced Mechanical and Chemical Durability: Driving of Alkali. *Appl. Surf. Sci.* 455, 115–122. doi:10.1016/j.apsusc.2018.05.169

Lin, W., Huang, Y., Li, J., Liu, Z., Yang, W., Li, R., et al. (2018). Preparation of Highly Hydrophobic and Anti-fouling wood Using Poly(methylhydrogen) siloxane. *Cellulose* 25, 7341–7353. doi:10.1007/s10570-018-2074-y

Montazer, M., Behzadnia, A., Pakdel, E., Rahimi, M. K., and Moghadam, M. B. (2011). Photo Induced Silver on Nano Titanium Dioxide as an Enhanced Antimicrobial Agent for Wool. *J. Photochem. Photobiol. B: Biol.* 103, 207–214. doi:10.1016/j.jphotobiol.2011.03.009

Pandit, S. K., Tudu, B. K., Mishra, I. M., and Kumar, A. (2020). Development of Stain Resistant, Superhydrophobic and Self-Cleaning Coating on wood Surface. *Prog. Org. Coat.* 139, 105453. doi:10.1016/j.porgcoat.2019.105453

Poncin-Epaillard, F., Herry, J. M., Marmey, P., Legeay, G., Debarnot, D., and Bellon-Fontaine, M. N. (2013). Elaboration of Highly Hydrophobic Polymeric Surface - A Potential Strategy to Reduce the Adhesion of Pathogenic Bacteria?. *Mater. Sci. Eng. C* 33, 1152–1161. doi:10.1016/j.msec.2012.12.020

Pouzet, M., Dubois, M., Charlet, K., and Béakou, A. (2018). From Hydrophilic to Hydrophobic wood Using Direct Fluorination: A Localized Treatment. *Comptes Rendus Chim.* 21, 800–807. doi:10.1016/j.crci.2018.03.009

Privett, B. J., Youn, J., Hong, S. A., Lee, J., Han, J., Shin, J. H., et al. (2011). Antibacterial Fluorinated Silica Colloid Superhydrophobic Surfaces. *Langmuir* 27, 9597–9601. doi:10.1021/la201801e

Shah, S. M., Zulfiqar, U., Hussain, S. Z., Ahmad, I., Habib-ur-Rehman, Hussain, I., et al. (2017). A Durable Superhydrophobic Coating for the protection of wood Materials. *Mater. Lett.* 203, 17–20. doi:10.1016/j.matlet.2017.05.126

Teacă, C. A., and Tanasa, F. (2020). Wood Surface Modification-Classic and Modern Approaches in wood Chemical Treatment by Esterification Reactions. *Coatings* 10, 1–31. doi:10.3390/coatings10070629

Thakur, K., Kalia, S., Kaith, B. S., Pathania, D., Kumar, A., Thakur, P., et al. (2016). The Development of Antibacterial and Hydrophobic Functionalities in Natural Fibers for Fiber-Reinforced Composite Materials. *J. Environ. Chem. Eng.* 4, 1743–1752. doi:10.1016/j.jece.2016.02.032

Tudu, B. K., Gupta, V., Kumar, A., and Sinhamahapatra, A. (2020a). Freshwater Production via Efficient Oil-Water Separation and Solar-Assisted Water Evaporation Using Black Titanium Oxide Nanoparticles. *J. Colloid Interf. Sci.* 566, 183–193. doi:10.1016/j.jcis.2020.01.079

Tudu, B. K., Sinhamahapatra, A., and Kumar, A. (2020b). Surface Modification of Cotton Fabric Using TiO2Nanoparticles for Self-Cleaning, Oil-Water Separation, Antistain, Anti-water Absorption, and Antibacterial Properties. *ACS Omega* 5, 7850–7860. doi:10.1021/acsomega.9b04067

Wang, J. Y., and Cooper, P. A. (2005). Effect of Oil Type, Temperature and Time on Moisture Properties of Hot Oil-Treated wood. *Holz Roh Werkst* 63, 417–422. doi:10.1007/s00107-005-0033-4

Wu, Y., Wu, X., Yang, F., Gan, J., and Jia, H. (2021). The Preparation of Cotton Fabric with Super-hydrophobicity and Antibacterial Properties by the Modification of the Stearic Acid. *J. Appl. Polym. Sci.* 138, 50717. doi:10.1002/app.50717

Wu, Y., Yang, L., Zhou, J., Yang, F., Huang, Q., and Cai, Y. (2020a). Softened wood Treated by Deep Eutectic Solvents. *ACS Omega* 5, 22163–22170. doi:10.1021/acsomega.0c02223

Wu, Y., Zhou, J., Huang, Q., Yang, F., Wang, Y., Liang, X., et al. (2020b). Study on the Colorimetry Properties of Transparent Wood Prepared from Six Wood Species. *ACS Omega* 5, 1782–1788. doi:10.1021/acsomega.9b02498

Xin, B., and Hao, J. (2010). Reversibly Switchable Wettability. *Chem. Soc. Rev.* 39, 769–782. doi:10.1039/b913622c

Xu, L., Wang, L., Shen, Y., Ding, Y., and Cai, Z. (2015). Preparation of Hexadecyltrimethoxysilane-Modified Silica Nanocomposite Hydrosol and Superhydrophobic Cotton Coating. *Fibers Polym.* 16, 1082–1091. doi:10.1007/s12221-015-1082-x

Yang, L., Wu, Y., Yang, F., and Wang, W. (2021). A Conductive Polymer Composed of a Cellulose-Based Flexible Film and Carbon Nanotubes. *RSC Adv.* 11, 20081–20088. doi:10.1039/d1ra03474j

Yang, T., Cao, J., and Ma, E. (2019). How Does Delignification Influence the Furfurylation of wood? *Ind. Crops Prod.* 135, 91–98. doi:10.1016/j.indcrop.2019.04.019

Yao, X., Song, Y., and Jiang, L. (2011). Applications of Bio-Inspired Special Wettable Surfaces. *Adv. Mater.* 23, 719–734. doi:10.1002/adma.201002689

Ye, R., Chyan, Y., Zhang, J., Li, Y., Han, X., Kittrell, C., et al. (2017). Laser-Induced Graphene Formation on Wood. *Adv. Mater.* 29, 1702211–1702217. doi:10.1002/adma.201702211

Zhang, Z., Liu, H., and Qiao, W. (2020). Reduced Graphene-Based Superhydrophobic Sponges Modified by Hexadecyltrimethoxysilane for Oil Adsorption. *Colloids Surf. A: Physicochemical Eng. Aspects* 589, 124433. doi:10.1016/j.colsurfa.2020.124433

Zhu, M., Song, J., Li, T., Gong, A., Wang, Y., Dai, J., et al. (2016). Highly Anisotropic, Highly Transparent Wood Composites. *Adv. Mater.* 28, 5181–5187. doi:10.1002/adma.201600427

Conflict of Interest: The authors declare that the research was conducted in the absence of any commercial or financial relationships that could be construed as a potential conflict of interest.